Resonant scattering of surface plasmon polaritons by dressed quantum dots

Danhong Huang, Michelle Easter, Godfrey Gumbs, A. A. Maradudin, Shawn-Yu Lin, Dave Cardimona, and Xiang Zhang

Articles you may be interested in

Transmission properties of surface plasmon polaritons and localized resonance in semiconductor hole arrays
Appl. Phys. Lett. **97**, 261111 (2010); 10.1063/1.3532111

Enhancement of emission from CdSe quantum dots induced by propagating surface plasmon polaritons
Appl. Phys. Lett. **94**, 173506 (2009); 10.1063/1.3114383

Spectral sensitivity of two-dimensional nanohole array surface plasmon polariton resonance sensor
Appl. Phys. Lett. **91**, 123112 (2007); 10.1063/1.2789181

Tunable resonance in surface-plasmon-polariton enhanced spontaneous emission using a denser dielectric cladding
Appl. Phys. Lett. **89**, 051916 (2006); 10.1063/1.2335506

Direct imaging of propagation and damping of near-resonance surface plasmon polaritons using cathodoluminescence spectroscopy
Appl. Phys. Lett. **88**, 221111 (2006); 10.1063/1.2208556

Resonant scattering of surface plasmon polaritons by dressed quantum dots

Danhong Huang,[1] Michelle Easter,[2] Godfrey Gumbs,[3] A. A. Maradudin,[4] Shawn-Yu Lin,[5] Dave Cardimona,[1] and Xiang Zhang[6]

[1]Air Force Research Laboratory, Space Vehicles Directorate, Kirtland Air Force Base, New Mexico 87117, USA
[2]Department of Mechanical Engineering, Stevens Institute of Technology, 1 Castle Point Terrace, Hoboken, New Jersey 07030, USA
[3]Department of Physics and Astronomy, Hunter College of the City University of New York, 695 Park Avenue, New York, New York 10065, USA
[4]Department of Physics and Astronomy, University of California, Irvine, California 92697, USA
[5]Department of Electrical, Computer and Systems Engineering, Rensselaer Polytechnic Institute, 110 8th Street, Troy, New York 12180, USA
[6]Department of Mechanical Engineering, 3112 Etcheverry Hall, University of California at Berkeley, Berkeley, California 94720, USA

The resonant scattering of surface plasmon-polariton waves (SPP) by embedded semiconductor quantum dots above the dielectric/metal interface is explored in the strong-coupling regime. In contrast to non-resonant scattering by a localized dielectric surface defect, a strong resonant peak in the spectrum of the scattered field is predicted that is accompanied by two side valleys. The peak height depends nonlinearly on the amplitude of SPP waves, reflecting the feedback dynamics from a photon-dressed electron-hole plasma inside the quantum dots. This unique behavior in the scattered field peak strength is correlated with the occurrence of a resonant dip in the absorption spectrum of SPP waves due to the interband photon-dressing effect. Our result on the scattering of SPP waves may be experimentally observable and applied to spatially selective illumination and imaging of individual molecules. © 2014 AIP Publishing LLC. [http://dx.doi.org/10.1063/1.4883859]

Most of the previous research carried out on the optical properties of condensed matter, including the optical absorption and inelastic light scattering, made use of a weak probe field as a perturbation to the system under investigation.[1] In this weak-coupling limit, the optical response of electrons depends only on the material characteristics. However, with increased field intensity, the optical properties of materials are found to depend nonlinearly on the strength of the external perturbation.[2]

The strong photon-electron interaction in semiconductors is known to produce dressed states[3–5] with a Rabi gap for electrons, and to create substantial nonlinearity in the semiconductor.[6–8] The presence of an induced polarization field, treated as a source term[9] arising from photo-excited electrons, allows for a *resonant* scattering of surface plasmon-polariton waves (SPP).[10] This is quite different from the *non-resonant* scattering of SPP waves by a localized dielectric surface defect[11,12] or by surface roughness.[13]

In this Letter, we report on a theoretical study dealing with the strong coupling between embedded semiconductor quantum dots and the electric field of SPPs, which has not been fully explored so far from either theoretically or experimentally. The conclusion on the scattering of SPP waves by photon dressed quantum dots may be experimentally observable. We demonstrate the possible control of interband optical response for semiconductor quantum dots by a strong electric field, like an optical gate, and provide a physical mechanism for near-field imaging beyond the optical diffraction limit.

Based on the analytical expression[14,15] for the Green's function of the coupled quantum dot and semi-infinite metallic material system, we report our semi-analytic solutions of the self-consistent equations for strongly coupled electromagnetic field dynamics and quantum kinetics of electrons

in a quantum dot above the surface of a thick metallic film. In our formalism, the strong light-electron interaction is manifested in the photon-dressed electronic states and the feedback from the induced optical polarization of dressed electrons to the incident light. Our results predict a strong resonant peak in the spectrum of the scattered field, which is accompanied by two side valleys. Furthermore, we discover that the peak height varies nonlinearly with the amplitude of the SPP waves. This demonstrates the effect of feedback dynamics from the photon-dressed electron-hole (e-h) plasma inside the quantum dots. Additionally, this unique observation in the spectrum of the scattered field is shown to correlate with a resonant dip observed in the absorption spectrum[10] of SPP waves, which is attributed to an effect of the interband photon-dressing of electronic states.

The results presented in this paper may be applied to the spatially selective illumination of individual molecules or neuron cells to control locally either low-temperature photo-excited chemical reactions or neuron firing activities in optogenetics and neuroscience. Although the coupling between excitons and light has been theoretically investigated previously, these studies were mostly limited to a simplified one-dimensional cavity or a perturbative approach, in contrast to the three-dimensional structure and self-consistent approach presented here. The formalism derived here goes beyond the weak-coupling limit and deals with a much more realistic structure in the strong-coupling limit for the development of a polariton laser with a very low threshold pumping.

Our model system consists of a semi-infinite metallic material and a semiconductor quantum dot above its surface. A SPP wave is locally excited through a surface grating by normally incident light. This propagating SPP wave further

excites an interband e-h plasma within the quantum dot. The induced local optical polarization field of the photo-excited e-h plasma is resonantly coupled to the SPP wave to produce a splitting in the degenerate e-h plasma and SPP modes with an anti-crossing gap.

By using the Green's function $\mathcal{G}_{\mu\nu}(\mathbf{r}, \mathbf{r}'; \omega)$, we may express Maxwell's equation for the electric field component $\boldsymbol{E}(\mathbf{r}; \omega)$ of an electromagnetic field in a semi-infinite non-magnetic medium in position-frequency space as an integral equation, i.e.,

$$E_\mu(\mathbf{r}; \omega) = E_\mu^{(0)}(\mathbf{r}; \omega)$$
$$- \frac{\omega^2}{\epsilon_0 c^2} \sum_\nu \int d^3\mathbf{r}' \, \mathcal{G}_{\mu\nu}(\mathbf{r}, \mathbf{r}'; \omega) \, \mathcal{P}_\nu^{\text{loc}}(\mathbf{r}'; \omega), \quad (1)$$

where $\boldsymbol{E}^{(0)}(\mathbf{r}; \omega)$ is a solution in the absence of semiconductor quantum dots, $\mathbf{r} = (x_1, x_2, x_3)$ is a position vector, ω is the light angular frequency, ϵ_0 and c are the permittivity and speed of light in vacuum, $\mathcal{P}^{\text{loc}}(\mathbf{r}; \omega)$ is an off-surface local polarization field that is generated by optical transitions of electrons in a quantum dot, which generally depends on the electric field in a nonlinear way and should be determined by the optical Bloch equations. Additionally, the position-dependent dielectric constant $\epsilon_b(x_3; \omega)$ is equal to ϵ_d for the semi-infinite dielectric material in the region $x_3 > 0$ but is given by $\epsilon_M(\omega)$ for the semi-infinite metallic material in the region $x_3 < 0$.

By assuming a SPP wave propagating along the x_1–x_2-plane, we can write the electric field of the incident SPP as

$$\boldsymbol{E}^{(0)}(\mathbf{r}; \omega_{\text{sp}}) = E_{\text{sp}} \, e^{i\mathbf{k}_0(\omega_{\text{sp}}) \cdot \mathbf{D}_0} \, \frac{c}{\omega_{\text{sp}}}$$
$$\times \left[i\hat{\mathbf{k}}_0 \beta_3(k_0, \omega_{\text{sp}}) - \hat{\mathbf{x}}_3 k_0(\omega_{\text{sp}}) \right]$$
$$\times e^{i\mathbf{k}_0(\omega_{\text{sp}}) \cdot \mathbf{x}_\parallel} \, e^{-\beta_3(k_0, \omega_{\text{sp}})x_3}, \quad (2)$$

where $\mathbf{x}_\parallel = \{x_1, x_2\}$, $\hat{\mathbf{k}}_0$ and $\hat{\mathbf{x}}_3$ are the unit vectors in the $\mathbf{k}_0 = k_0(\omega_{\text{sp}})\{\cos\theta_0, \sin\theta_0\}$ and x_3 directions, E_{sp} is the field amplitude, ω_{sp} is the field frequency, θ_0 is the angle of the incident SPP wave with respect to the x_1 direction, $\mathbf{D}_0 = \{-x_{1g}, -x_{2g}\}$ is the position vector of the center of a surface grating, and the two wave numbers in Eq. (2) are given by

$$k_0(\omega_{\text{sp}}) = \frac{\omega_{\text{sp}}}{c} \sqrt{\frac{\epsilon_d \, \epsilon_M(\omega_{\text{sp}})}{\epsilon_d + \epsilon_M(\omega_{\text{sp}})}} \quad (3)$$

and

$$\beta_3(k_0, \omega_{\text{sp}}) = \sqrt{k_0^2(\omega_{\text{sp}}) - \frac{\omega_{\text{sp}}^2}{c^2}}, \quad (4)$$

with $\text{Re}[k_0(\omega_{\text{sp}})] \geq 0$ and $\text{Re}[\beta_3(k_0, \omega_{\text{sp}})] \geq 0$. Here, the in-plane wave vector k_0 is produced by the surface-grating

diffraction of the p-polarized normally incident light, which in turn determines the resonant frequency ω_{sp} of the surface plasmon-polariton mode. Here, the exact dispersion relation for the SPP field is provided by Eq. (3), which includes both the radiative and the non-radiative parts. For the resonant scattering of the SPP near field, only the non-radiative part of the dispersion relation needs to be considered. The general review of non-resonant light scattering can be found from Ref. 16.

In order for us to explicitly determine the electric field dependence of $\mathcal{P}^{\text{loc}}(\mathbf{r}; \omega)$, we now turn to the quantum kinetics of electrons in a quantum dot. Here, the optical polarization field $\mathcal{P}^{\text{loc}}(\mathbf{r}; \omega)$ plays a unique role in bridging the gap between the classical Maxwell's equations for electromagnetic fields and the quantum-mechanical Schrödinger equation for electrons. The quantum kinetics of electrons in photo-excited quantum dots should be adequately described by the semiconductor Bloch equations (SBEs),[6–8] which are a generalization of the well-known optical Bloch equations in two ways, namely, in their incorporation of electron scattering, as well as their inclusion of many-body effects on dephasing.

For photo-excited spin-degenerate electrons (holes) in the conduction (valence) band, the SBEs with $\ell(j) = 1, 2, \ldots$ are given, within the rotating-wave approximation, by

$$\frac{dn_{\ell(j)}^{\text{e(h)}}}{dt} = \frac{2}{\hbar} \sum_{j(\ell)} \text{Im}\left[\left(Y_\ell^j\right)^* \left(\mathcal{M}_{\ell,j}^{\text{eh}} - Y_\ell^j V_{\ell,j;j,\ell}^{\text{eh}}\right) \right]$$
$$+ \left.\frac{\partial n_{\ell(j)}^{\text{e(h)}}}{\partial t}\right|_{\text{rel}} - \delta_{\ell(j),1} \, \mathcal{R}_{\text{sp}} \, n_1^{\text{e}} \, n_1^{\text{h}}, \quad (5)$$

where $\mathcal{R}_{\text{sp}}$ is the spontaneous emission rate, which should be calculated by using the Kubo-Martin-Schwinger relation[17] and including band gap energy and interband dipole moment renormalizations, and $n_{\ell(j)}^{\text{e(h)}}$ represents the electron (hole) level population. In Eq. (5), the Boltzmann-type scattering term for non-radiative energy relaxation of electrons (holes) is $\left.\frac{\partial n_{\ell(j)}^{\text{e(h)}}}{\partial t}\right|_{\text{rel}} = \mathcal{W}_{\ell(j)}^{\text{in}}(1 - n_{\ell(j)}^{\text{e(h)}}) - \mathcal{W}_{\ell(j)}^{\text{out}} n_{\ell(j)}^{\text{e(h)}}$, where $\mathcal{W}_{\ell(j)}^{\text{in}}$ and $\mathcal{W}_{\ell(j)}^{\text{out}}$ are the scattering-in and scattering-out rates for electrons (holes), respectively, and should be calculated by including carrier-carrier and carrier-(optical) phonon interactions. Moreover, we know from Eq. (5) that the total number $N_{\text{e(h)}}(t)$ of photo-excited electrons (holes) is conserved in the absence of recombination. Here, the rotating-wave approximation can be justified for steady states if the frequency of the SPP field is resonant with the electron interband transition in the quantum dot and the size of the quantum dot is much smaller than the wavelength of the SPP field.

The induced optical polarization in the SBEs with $\ell(j) = 1, 2, \ldots$ satisfies the following equations for a spin-averaged e-h plasma:

$$i\hbar \frac{d}{dt} Y_\ell^j = \left[\bar{\varepsilon}_\ell^{\text{e}}(\omega|t) + \bar{\varepsilon}_j^{\text{h}}(\omega|t) - \hbar(\omega + i\gamma_0) \right] Y_\ell^j + \left(1 - n_\ell^{\text{e}} - n_j^{\text{h}}\right) \left(\mathcal{M}_{\ell,j}^{\text{eh}} - Y_\ell^j V_{\ell,j;j,\ell}^{\text{eh}} \right)$$
$$+ Y_\ell^j \left[\sum_{j_1} n_{j_1}^{\text{h}} \left(V_{j,j_1;j_1,j}^{\text{hh}} - V_{j,j_1;j,j_1}^{\text{hh}} \right) - \sum_{\ell_1} n_{\ell_1}^{\text{e}} V_{\ell,j;j,\ell_1}^{\text{eh}} \right] + Y_\ell^j \left[\sum_{\ell_1} n_{\ell_1}^{\text{e}} \left(V_{\ell,\ell_1;\ell_1,\ell}^{\text{ee}} - V_{\ell,\ell_1;\ell,\ell_1}^{\text{ee}} \right) - \sum_{j_1} n_{j_1}^{\text{h}} V_{\ell,j_1;j_1,\ell}^{\text{eh}} \right], \quad (6)$$

where Y_ℓ^j represents the induced interband optical coherence, $\hbar\gamma_0 = \hbar\gamma_{eh} + \hbar\gamma_{ext}$ is the energy level broadening (due to the finite carrier lifetime plus the radiation loss of an external evanescent field), $\bar{\varepsilon}_{\ell(j)}^{e(h)}(\omega|t)$ is the kinetic energy of dressed single electrons (holes) (see supplementary material for *electronic states of a quantum dot*).[20] In Eq. (6), the diagonal dephasing of Y_ℓ^j, the renormalization of interband Rabi coupling, the renormalization of electron and hole energies, as well as the exciton binding energy, are all taken into account. Since the e-h plasma is not spin-dependent, they may be excited by both left and right circularly polarized light. The off-diagonal dephasing of Y_ℓ^j has been neglected due to the low carrier density in quantum dots. In Eqs. (5) and (6), we have introduced the Coulomb matrix elements $V_{\ell_1,\ell_2;\ell_3,\ell_4}^{ee}$, $V_{j_1,j_2;j_3,j_4}^{hh}$ and $V_{\ell,j;j',\ell'}^{eh}$, for electron-electron, hole-hole, and e-h interactions, respectively.

The steady-state solution of Eq. (6), i.e., subject to the condition that $dY_\ell^j/dt = 0$, has been obtained as

$$Y_\ell^j(t|\omega) = \left[\frac{1 - n_\ell^e(t) - n_j^h(t)}{\hbar(\omega + i\gamma_0) - \hbar\bar{\Omega}_{\ell,j}^{eh}(\omega|t)}\right]\mathcal{M}_{\ell,j}^{eh}(t), \qquad (7)$$

where the photon and Coulomb renormalized interband energy level separation $\hbar\bar{\Omega}_{\ell,j}^{eh}(\omega|t)$ is given by

$$\begin{aligned}
\hbar\bar{\Omega}_{\ell,j}^{eh}(\omega|t) =\ & \bar{\varepsilon}_\ell^e(\omega|t) + \bar{\varepsilon}_j^h(\omega|t) - V_{\ell,j;j,\ell}^{eh} \\
& + \sum_{\ell_1} n_{\ell_1}^e(t)(V_{\ell,\ell_1;\ell_1,\ell}^{ee} - V_{\ell,\ell_1;\ell,\ell_1}^{ee}) + \sum_{j_1} n_{j_1}^h(t) \\
& \times (V_{j,j_1;j_1,j}^{hh} - V_{j,j_1;j,j_1}^{hh}) - \sum_{\ell_1 \neq \ell} n_{\ell_1}^e(t)V_{\ell_1,j;j,\ell_1}^{eh} \\
& - \sum_{j_1 \neq j} n_{j_1}^h(t)V_{\ell,j_1;j_1,\ell}^{eh}
\end{aligned} \qquad (8)$$

and the matrix elements employed in Eqs. (5) and (6) for the Rabi coupling between photo-excited carriers and an evanescent pump field $\boldsymbol{E}(\mathbf{r}; t) = \theta(t)\boldsymbol{E}(\mathbf{r}; \omega)e^{-i\omega t}$ are given by

$$\mathcal{M}_{\ell,j}^{eh}(t) = -\delta_{\ell,1}\,\delta_{j,1}\,\theta(t)\,[\boldsymbol{E}_{\ell,j}^{eh}(\omega) \cdot \mathbf{d}_{c,v}]. \qquad (9)$$

In this notation, $\theta(x)$ is the Heaviside unit step function, the static interband dipole moment denoted by $\mathbf{d}_{c,v}$ is given by Refs. 18 and 19 (see supplementary material for *electronic states of a quantum dot*)[20]

$$\mathbf{d}_{c,v} = \int d^3\mathbf{r}[u_c(\mathbf{r})]^*\,\mathbf{r}\,u_v(\mathbf{r}) = \mathbf{d}_{c,v}^*, \qquad (10)$$

where $u_c(\mathbf{r})$ and $u_v(\mathbf{r})$ are the Bloch functions associated with conduction and valence bands at the Γ-point in the first Brillouin zone of the host semiconductor, and the effective electric field coupled to the quantum dot is evaluated by

$$\boldsymbol{E}_{\ell,j}^{eh}(\omega) = \int d^3\mathbf{r}[\psi_\ell^e(\mathbf{r})]^*\boldsymbol{E}(\mathbf{r}; \omega)[\psi_j^h(\mathbf{r})]^*, \qquad (11)$$

where $\psi_{\ell(j)}^{e(h)}(\mathbf{r})$ is the envelope function of electrons (holes) in the quantum dot. Next, the photo-induced interband optical polarization $\mathcal{P}^{loc}(\mathbf{r}; \omega)$ by dressed electrons in the quantum dot is given by[2]

$$\begin{aligned}
\mathcal{P}^{loc}(\mathbf{r}; \omega) =\ & 2|\xi_{QD}(\mathbf{r})|^2\,\mathbf{d}_{c,v}\left\{\int d^3\mathbf{r}'\,\psi_1^e(\mathbf{r}')\,\psi_1^h(\mathbf{r}')\right\} \\
& \times \frac{1}{\hbar}\lim_{t\to\infty}\left[\frac{1 - n_1^e(t) - n_1^h(t)}{\omega + i\gamma_0 - \bar{\Omega}_{1,1}^{eh}(\omega|t)}\right]\mathcal{M}_{1,1}^{eh}(t), \quad (12)
\end{aligned}$$

where the profile function $|\xi_{QD}(\mathbf{r})|^2$ comes from the quantum confinement inside a quantum dot.

In our numerical calculations, we chose the quantum dot dimensions as $210\,\text{Å}$ and $100\,\text{Å}$ along the x and y directions, respectively, $m_e^* = 0.067\,m_0$ and $m_h^* = 0.62\,m_0$ for the electron and hole effective masses, in terms of the free electron mass m_0, $\theta_0 = 45°$, $x_{1g} = x_{2g} = 610\,\text{Å}$, $\epsilon_b = 12$ for the quantum dot, $\epsilon_d = 12$ for the cladding layer, $\epsilon_s = 11$ and $\epsilon_\infty = 13$ for the static and optical dielectric constants, $\hbar\Omega_0 = 36\,\text{meV}$ for the energy of optical phonons, $\hbar\Gamma_{ph} = 3\,\text{meV}(=\hbar\gamma_0)$ for the phonon broadening, $z_0 = 610\,\text{Å}$, and $T = 300\,\text{K}$ for the lattice temperature. The silver plasma frequency is $13.8 \times 10^{15}\,\text{Hz}$, and the silver plasma dephasing parameter is $0.1075 \times 10^{15}\,\text{Hz}$. The energy gap E_G for the active quantum-dot material is $1.927\,\text{eV}$ at $T = 300\,\text{K}$. Here, the ratio of z_0 to the light wavelength in vacuum is about 0.1, which ensures that the SPP near field will not be quenched.

Figure 1 presents the absorption coefficient $\beta_0(\omega_{sp})$ for an SPP wave by a quantum dot,[17] the scattered field $|\mathbf{E}_{tot} - \mathbf{E}_{sp}|$ of the SPP wave, and the energy-level occupations for electrons $n_{\ell,e}$ and holes $n_{j,h}$ with $\ell, j = 1, 2$ as functions of the frequency detuning $\Delta\hbar\omega_{sp} \equiv \hbar\omega_{sp} - (E_G + \varepsilon_{1,e} + \varepsilon_{1,h})$ with bare energies $\varepsilon_{1,e}, \varepsilon_{1,h}$ for ground-state electrons and holes. A dip is observed at resonance, when $\Delta\hbar\omega_{sp} = 0$, in Fig. 1(a), which becomes deeper with decreasing amplitude E_{sp} of the SPP wave in the strong-coupling regime due to a reduction of saturated absorption. However, this dip disappears when E_{sp} drops to $25\,\text{kV/cm}$ in the weak-coupling limit due to the suppression of the photon dressing effect, which is accompanied by a one-order of magnitude increase in the absorption-peak strength. The dip in Fig. 1(a) corresponds to a peak in the scattered field, as may be seen from Fig. 1(b). The scattered field increases with the frequency detuning away from resonance, corresponding to decreasing absorption. Consequently, two local minima appear on both sides of the resonance for the scattered field in the strong-coupling regime. The Maxwell-Bloch equations couple the field dynamics outside a quantum dot with the electron dynamics inside the dot. At $E_{sp} = 125\,\text{kV/cm}$ in Fig. 1(d), we obtain peaks in energy-level occupations at resonance, which are broadened by the finite carrier lifetime, as well as by the optical power of the SPP wave. Moreover, jumps in the energy level occupation may be seen at resonance due to the Rabi splitting of the energy levels in the dressed electron states. The effect of resonant phonon absorption also plays a significant role in the finite value of $n_{2,e}$ with energy-level separations $\varepsilon_{2,e} - \varepsilon_{1,e} \approx \hbar\Omega_0$. However, as E_{sp} decreases to $25\,\text{kV/cm}$ in Fig. 1(c), peaks in the energy-level occupations are greatly sharpened and negatively shifted due to the suppression of the broadening from the optical power and the excitonic effect, respectively. Additionally, jumps in the energy level occupations become invisible because the Rabi-split energy gap in this case is much smaller than the
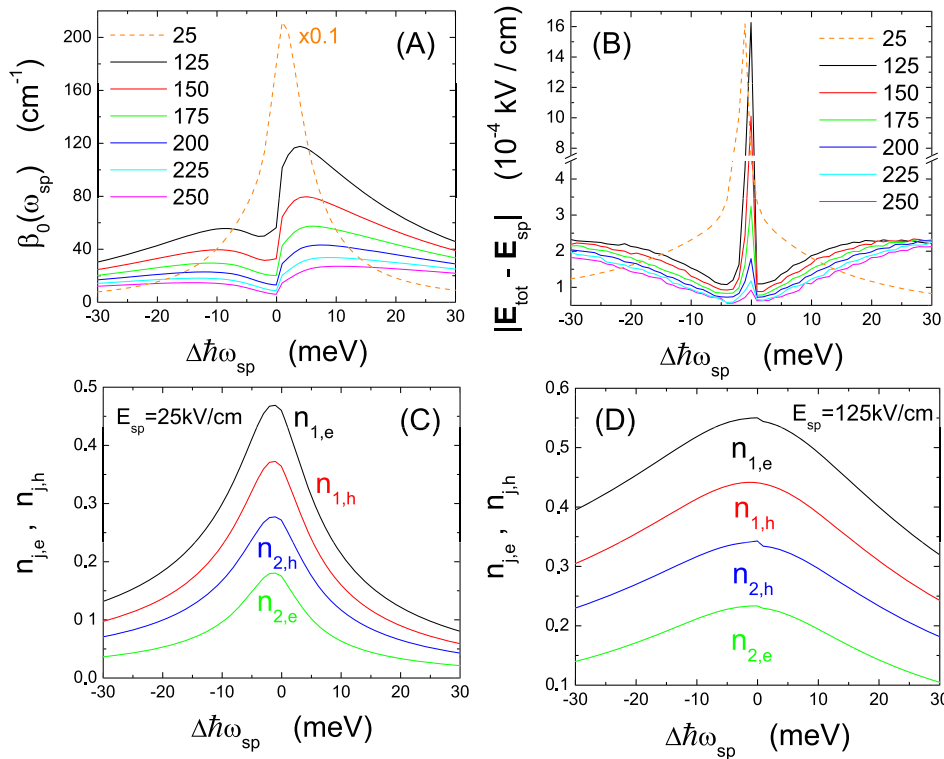
FIG. 1. Absorption coefficients $\beta_0(\omega_{sp})$ (a) and scattered field $|\mathbf{E}_{tot} - \mathbf{E}_{sp}|$ at the quantum dot (b), as well as the energy-level occupations for electrons $n_{\ell,e}$ and holes $n_{j,h}$ [(c) and (d)] as functions of the frequency detuning $\Delta\hbar\omega_{sp} = \hbar\omega_{sp} - (E_G + \varepsilon_{1,e} + \varepsilon_{1,h})$. The results for various amplitudes E_{sp} of an SPP wave with frequency ω_{sp} are presented in (a) and (b), along with a comparison of the energy-level occupations for $E_{sp} = 25$ and $125\,\text{kV/cm}$ in (c) and (d). The label $\times 0.1$ in (a) indicates that the result is multiplied by a factor of 0.1.

energy-level broadening from the finite lifetime of electrons (i.e., substantially damped Rabi oscillations between the first electron and hole levels).
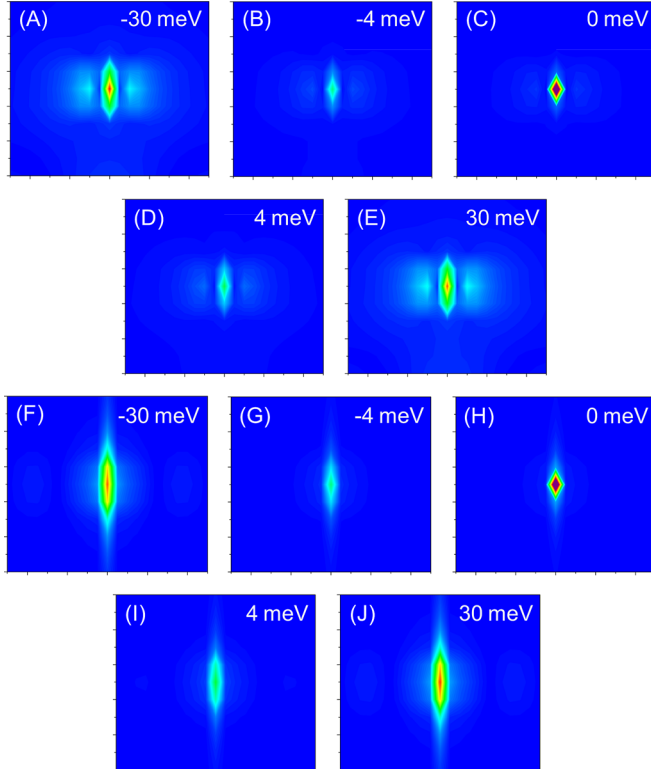

FIG. 2. Scattered field color maps for $|E^\nu_{tot} - E^\nu_{sp}|/E_{sp}$ (with $y = 0$) around a quantum dot above a metallic surface in the x [$\nu = 1$, (a)–(e)] and z [$\nu = 3$, ((f)–(j)] directions, respectively, with varying frequency detuning $\Delta\hbar\omega_{sp} = -30, -4, 0, 4$, and $30\,\text{meV}$. We chose $E_{sp} = 15\,\text{kV/cm}$. The color scales (blue-to-red) for all values of $\Delta\hbar\omega_{sp}$ are $0 - 1 \times 10^{-7}$ in (a)–(e) and $0 - 1.6 \times 10^{-6}$ in (f)–(j) except for $\Delta\hbar\omega_{sp} = 0$ where the color scales are $0 - 4.5 \times 10^{-7}$ in (c) and $0 - 7 \times 10^{-6}$ in (h).

Although the interband dipole moment of a quantum dot is isotropic in space, the scattered field (see Fig. 2 with $E_{sp} = 150\,\text{kV/cm}$) in the x direction [Figs. 2(a)–2(e)] and in the z direction [Figs. 2(f)–2(j)] are still different due to the presence of a metallic surface perpendicular to the z direction in our system. However, this isotropic intensity distribution is mostly recovered at $\Delta\hbar\omega_{sp} = 0$. Specifically, the scattered field in the z direction is one order of magnitude larger than that in the x direction. The field pattern in Figs. 2(f)–2(h) tends to spread in the z direction, while the pattern in Figs. 2(a)–2(e) distributes in the x direction. From this figure, we also find that the intensities in both directions follow the pattern of strong-weak-strong-weak-strong as the frequency detuning is swept across $\Delta\hbar\omega_{sp} = 0$, which agrees with the observation of the scattered field at the quantum dot in Fig. 1(b).

Color maps for the scattered field around a quantum dot displayed in Fig. 2 are for strong coupling between the dot and an SPP wave. We present in Fig. 3 the scattered field maps in the weak-coupling regime, where the strong-weak-strong-weak-strong pattern in the strong-coupling regimes has been changed to a weak-strong-weak pattern. Moreover, the SPP-wave frequency for the resonant scattered field has been shifted from $\Delta\hbar\omega_{sp} = 0$ to $\Delta\hbar\omega_{sp} = 1\,\text{meV}$, demonstrating a positive depolarization shift of the optical excitation energy, as may be verified from Fig. 1(a). However, this depolarization effect is completely masked by the occurrence of a local minimum at $E_{sp} = 150\,\text{kV/cm}$.

In conclusion, for a strong SPP wave, we demonstrated its unique resonant scattering by a dynamical semiconductor quantum dot very close to the metal/dielectric interface. We also predicted correlation between a resonant peak in the scattered field spectrum and a resonant local minimum in the absorption spectrum of the SPP wave.

Although we investigated only the coupling between an SPP wave and a single quantum dot, our formalism may be
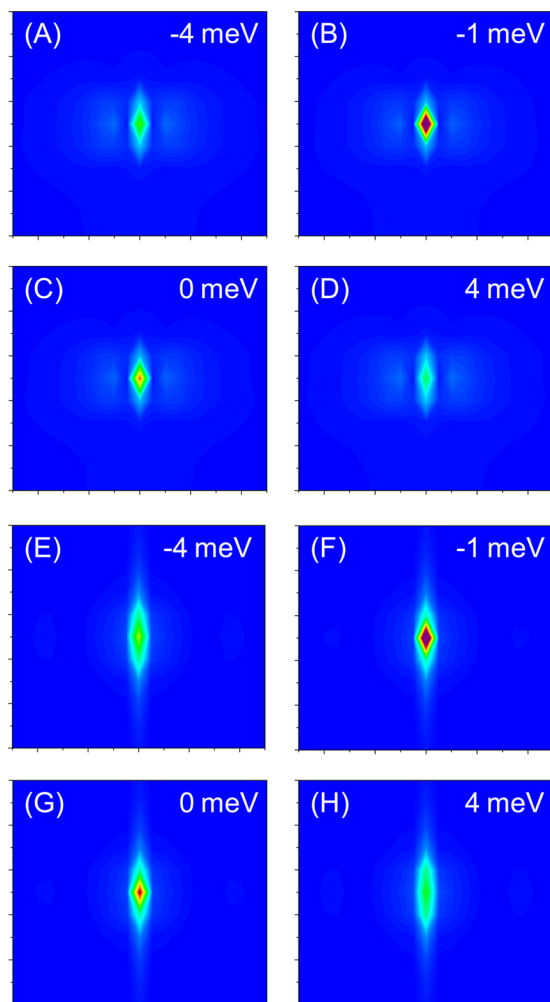
FIG. 3. Scattered field color maps for $|E_{tot}^\nu - E_{sp}^\nu|/E_{sp}$ (with $y = 0$) around a quantum dot above the metallic surface in the x [$\nu = 1$, (a)–(d)] and z [$\nu = 3$, (e)–(h)] directions, respectively, with varying frequency detuning $\Delta\hbar\omega_{sp} = -4, -1, 0,$ and 4 meV. Here, $E_{sp} = 25$ kV/cm is assumed. The color scales (blue-to-red) for all values of $\Delta\hbar\omega_{sp}$ are $0 - 1.4 \times 10^{-6}$ in (a)–(d) and $0 - 2 \times 10^{-5}$ in (e)–(h) except for $\Delta\hbar\omega_{sp} = -1$ meV where the color scales are $0 - 4 \times 10^{-6}$ in (b) and $0 - 7 \times 10^{-5}$ in (f).

generalized to include multiple quantum dots. The open surface of the metallic film provides an easy solution to perform biochemical and biomedical tests under a microscope in a laboratory setting. If the quantum dots are coated with

specially selected chemically reactive molecules, they may be able to adhere to special target tissue if the chemical properties are matched with each other. Therefore, the spontaneous emission by electrons in these quantum dots may be employed non-invasively for near-field imaging of target tissue with very high brightness and spatial resolution.

Additionally, instead of coupling to the lowest pair of e-h energy levels, we may choose the surface plasmon frequency for a resonant coupling to the next pair of e-h levels. In this case, optical pumping from the localized surface plasmon field may transfer a population inversion from the excited pair to the ground pair of e-h levels by emitting phonons, leading to possible lasing action. Such a surface plasmon based quantum-dot laser would have a beam size as small as a few nanometers, which is expected to be very useful for spatially selective illumination of individual neuron cells in optogenetics and neuroscience.

[1]G. Gumbs and D. H. Huang, *Properties of Interacting Low-Dimensional Systems* (Wiley-VCH Verlag GmbH & Co. kGaA, Weinheim, 2011), Chaps. 4, 5.
[2]S. Schmitt-Rink, D. S. Chemla, and H. Haug, Phys. Rev. B **37**, 941 (1988).
[3]D. Dini, R. Köhler, A. Tredicucci, G. Biasiol, and L. Sorba, Phys. Rev. Lett. **90**, 116401 (2003).
[4]Y. Todorov, A. M. Andrews, I. Sagnes, R. Colombelli, P. Klang, G. Strasser, and C. Sirtori, Phys. Rev. Lett. **102**, 186402 (2009).
[5]Y. Todorov, A. M. Andrews, R. Colombelli, S. De Liberato, C. Ciuti, P. Klang, G. Strasser, and C. Sirtori, Phys. Rev. Lett. **105**, 196402 (2010).
[6]F. Rossi and T. Kuhn, Rev. Mod. Phys. **74**, 895 (2002).
[7]V. M. Axt and T. Kuhn, Rep. Prog. Phys. **67**, 433 (2004).
[8]M. Kira and S. W. Koch, Prog. Quantum Electron. **30**, 155 (2006).
[9]F. Jahnke, M. Kira, and S. W. Koch, Z. Angew. Phys. B **104**, 559 (1997).
[10]J. A. Sánchez-Gil and A. A. Maradudin, Opt. Express **12**, 883 (2004).
[11]R. E. Arias and A. A. Maradudin, Opt. Express **21**, 9734 (2013).
[12]F. Pincemin, A. Sentenac, and J.-J. Greffet, J. Opt. Soc. Am. A **11**, 1117 (1994).
[13]A. A. Maradudin and D. L. Mills, Ann. Phys. **100**, 262 (1976).
[14]A. A. Maradudin and D. L. Mills, Phys. Rev. B **11**, 1392 (1975).
[15]M. G. Cottam and A. A. Maradudin, "Surface linear response functions," in *Surface Excitations*, edited by V. M. Agranovich and R. Loudon (North-Holland, Amsterdam, 1984), pp. 1–194.
[16]*Light Scattering and Nanoscale Surface Roughness*, edited by A. A. Maradudin (Springer, New York, 2007).
[17]D. H. Huang and P. M. Alsing, Phys. Rev. B **78**, 035206 (2008).
[18]E. O. Kane, J. Phys. Chem. Solids **1**, 249 (1957).
[19]U. Bockelmann and G. Bastard, Phys. Rev. B **45**, 1688 (1992).
[20]See supplementary material at http://dx.doi.org/10.1063/1.4883859 for electronic states of a quantum dot.